Full paper/Mémoire

Synthesis, characterization, and biological activity of some complex combinations of nickel with α-ketoglutaric acid and 1-(o-tolyl)biguanide

Mădălina Mihalache [a, *], Ovidiu Oprea [a], Cornelia Guran [a], Alina M. Holban [b]

[a] Department of Inorganic Chemistry, Chemistry-Physics and Electrochemistry, Faculty of Applied Chemistry and Materials Science, University Politehnica of Bucharest, 1 — 7 Polizu Str., 011061 Bucharest, Romania
[b] Department of Microbiology and Immunology, Faculty of Biology, University of Bucharest, Aleea Portocalelor, No. 1-3, Bucharest 060101, Romania

ARTICLE INFO

ABSTRACT

The four divalent nickel complexes having α-ketoglutaric acid (H_2A) and 1-(o-tolyl) biguanide (TB) ligands have been synthesized, characterized, and tested for antibacterial and antitumor activity.

The proposed formulas for these complexes are $[Ni(TB)(HA)(H_2O)_2]Cl$ (**C1**), $[Ni(TB)(HA)(H_2O)_2]Br$ (**C2**), $[Ni(TB)(HA)]NO_3 \cdot H_2O$ (**C3**), and $[Ni(TB)(HA)]CH_3COO$ (**C4**), where HA represents deprotonated H_2A.

For the four complexes and for the ligands used in the synthesis, the antibacterial activity against *Staphylococcus aureus* ATCC 25923 and *Pseudomonas aeruginosa* ATCC 27853 and antitumor activity in HeLa tumor cells were tested. A moderate cytotoxic effect of **C3** and **C4** complexes has been observed on the development and metabolic activity of HeLa cells, whereas **C1** and **C2** ligands have a very low effect on them.

The synthesized complexes (obtained) inhibit adherence to the inert substrate of bacterial strains *S. aureus* and *P. aeruginosa*; therefore, they may be candidates for (potential) therapeutic applications.

© 2017 Académie des sciences. Published by Elsevier Masson SAS. All rights reserved.

1. Introduction

Biguanides are compounds of importance due to their biological properties, of which worth to be mentioned are the antimicrobial, antifungal, antibacterial, hypoglycemic, antimalarial, and antitumor activities [1—8]. The special interest in studying the coordination complexes in which the ligand is of biguanide type is given by the fact that many of them possess biological properties.

Thus, complexes of Fe(III), Ni(II), and Cu(II) with *N,N*-dimethylbiguanide ligands and their derivatives $[Fe(DMBG)_2]Cl \cdot 0.5H_2O$, $[FeO(DMBG)_2]$, $[Ni(DMBG)_2]$, $[Cu(DMBG)_2] \cdot H_2O$, where HDMBG = N,N-dimethylbiguanide [9—11], $[Cu(HTBG)_2]Cl_2$ and $[Cu(TBG)_2] \cdot 3H_2O$, where HTBG is 2-tolylbiguanide [12], are known.

Biological, spectral, and molecular docking studies of 1-(o-tolyl)biguanide demonstrated its antimicrobial activity [13].

α-Ketoglutaric acid plays an essential role in the Krebs cycle; α-ketoacids are very important agents in the synthesis and degradation of amino acids and proteins in the metabolism of lipids and carbohydrates [14]. Studies on α-ketoacids with biological activity have shown that they can produce different effects on the biological tissue, interacting at the cellular level at different pH values, temperatures, and enzyme-controlled medium [15—17].

α-Ketoglutaric acid antagonizes toxic effects against both HCN and NaCN [18,19]. It has also a neuroprotective effect, helps in the healing and regeneration of tissues, in the development of the gastrointestinal tract, in lung disorders, and some types of cancer [14].

Complexes with lanthanides containing α-ketoglutaric acid as ligand have been synthesized [20].

Complexes with formula $[M_2(III)M(II)L_6(NO_3)_6(OH_2)_6]$ (NO_3), where M(III) = Ce and M(II) = Cu, Co, Ni, and L is α-ketoglutaric acid, have antibacterial properties and antioxidant activity [21].

Taking into account the biological properties of α-ketoglutaric acid and 1-(o-tolyl)biguanide, we aimed to synthesize and afterward study the properties of new complex combinations of Ni(II) with these ligands.

2. Experimental section

2.1. Materials and methods

The substances used to obtain the four complexes were of high purity and came from Alfa Aesar (α-ketoglutaric acid—$C_5H_6O_5$) and Sigma—Aldrich (1-(o-tolyl)biguanide—$C_9H_13N_5$, $NiCl_2 \cdot 6H_2O$, $NiBr_2$, $Ni(NO_3)_2 \cdot 6H_2O$, $Ni(CH_3COO)_2 \cdot 4H_2O$, and ethanol).

For synthesis of complex combinations, the substances used (nickel salts and two ligands) were dissolved in ethanol. Reactions occurred at approximately 40 °C under agitation. The complexes obtained were vacuum filtered, washed with ethanol, and dried with ethyl ether. The molar ratio of metal salts/α-ketoglutaric acid/1-(o-tolyl) biguanide was 1:1:1 using 1 mmol of each substance (0.1461 g $C_5H_6O_5$, 0.1913 g $C_9H_13N_5$, 0.2377 g $NiCl_2 \cdot 6H_2O$, 0.2185 g $NiBr_2$, 0,2908 g $Ni(NO_3)_2 \cdot 6H_2O$, and 0.2488 g $Ni(CH_3COO)_2 \cdot 4H_2O$). Synthesis of complex combinations led to pure compounds, which did not require further purification.

The nitrogen, carbon, and hydrogen content of the synthesized complexes was determined by microcombustion using a Flash 2000 Organic Elemental Analyzer. The presence of chlorine in complex **C1** was revealed with $AgNO_3$, and the percentage of nickel was determined using a Perkin Elmer AAnalyst 400 atomic absorption spectrometer.

Electronic spectra were recorded using a Jasco V670 spectrometer by the diffuse reflection method at room temperature in the range 200—1500 nm, using MgO as a standard.

A Nicolet IS 50 FT-IR spectrophotometer was used for recording FT-IR spectra in the 4000—200 cm^{-1} range. Thermal analysis was performed with a simultaneous thermogravimetric analysis/differential scanning calorimetry (TGA/DSC) STA 449 F1 Jupiter working in a dynamic air atmosphere at a flow rate of 20 mL/min in the range 25—900 °C with a heating rate of 10 °C/min. The molar electrical conductivity was determined using a CyberScan PCD 6500 conductivity meter in 10^{-3} M of *N,N*-dimethylformamide solution at 25 °C. Magnetic susceptibility was measured with a Gouy balance using the Faraday method and $Hg[Co(SCN)_4]$ as a calibrant.

Antitumor activity was tested in HeLa tumor cells using the MTT (3-(4,5-dimethylthiazol-2-yl)-2,5-diphenyltetra

zolium bromide) assay at a concentration of 500 μg/mL for 24 h incubation at 37 °C in 5% CO_2 atmosphere. The method is based on the following: under certain conditions, NAD(P)H-dependent cellular oxidoreductases may reflect the number of viable cells in a culture. These enzymes may reduce the MTT tetrazolium reagent to violet insoluble formazan (Fig. 1). The color intensity of formazan was evaluated by measuring optical density at a wavelength of 570 nm using a Filter Max F5 Multi-Mode Microplate Reader spectrophotometer.

The tetrazolium dye reduction method is often used to measure the cytotoxicity of some compounds and cell proliferation. Because MTT reagent is sensitive to light, the whole procedure is done in the dark.

The antibacterial activity of ligands and complexes synthesized was determined in vitro against *Pseudomonas aeruginosa* and *Staphylococcus aureus* bacterial strains. To determine the minimum inhibitory concentration (MIC), the broth microdilution method was used by successively diluting a 10 mg/mL complex combination solution using 96-well plates. According to the dilution scheme of complex compounds, the influence of a diluted dimethyl sulfoxide (DMSO) solvent was also quantified.

To determine the influence of the test compounds on the adhesion of a microbial biofilm to the inert substrate, the microbial cells were cultivated in the presence of compounds of interest into nutrient broth using 96-well plates. They were incubated at 37 °C for 24 h. The plates were emptied and washed twice with physiological sterile water, and the adhered cells were fixed with 0.1 mL of 80% methanol for 5 min. The methanol solution was removed by overturning, and the adhered cells were stained with 1% crystal violet alkaline solution (0.1 mL/well) for 15 min. The staining solution was removed and then the plates were washed under water stream. The microbial biofilms formed on the plastic plates were converted into suspension by bubbling in 33% acetic acid. The intensity of the suspension color was evaluated by measuring the absorbance at 492 nm using a Max F5 Multi-Mode Microplate Reader.

3. Results and discussion

3.1. Elemental analysis

To establish the formulas of coordination compounds that were synthesized, elemental analysis was performed. A good concordance between calculated and experimental percents of carbon, nitrogen, hydrogen, and nickel was found (Table 1).

3.2. Thermal analysis

On the basis of the interpretation of the results of the TGA, information has been obtained that has contributed to the proposed formulations for coordination complexes, namely, the presence of water molecules and the thermal effects associated with mass loss processes. Thermogravimetric (TG) and DSC curves of the four complexes are presented in Fig. 2(a—d).

From the analysis of the **C1** complex TG and DSC curves, the first decomposition step (<180 °C) indicates the loss of
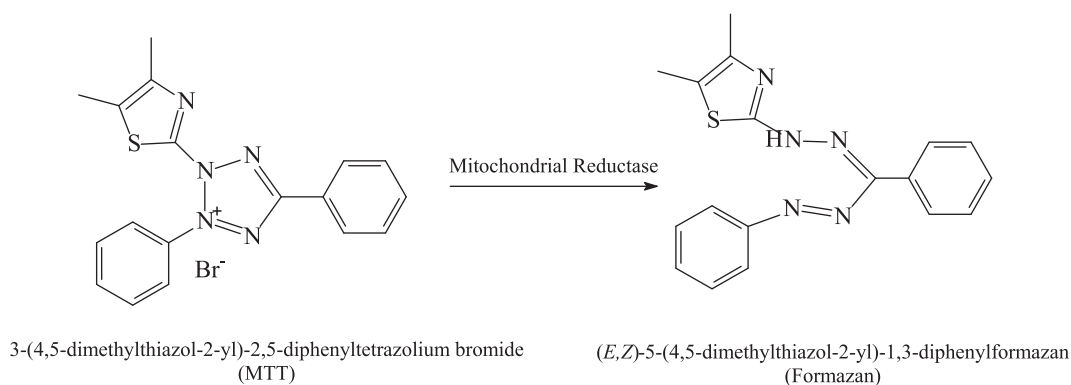
3-(4,5-dimethylthiazol-2-yl)-2,5-diphenyltetrazolium bromide (MTT) → Mitochondrial Reductase → (*E,Z*)-5-(4,5-dimethylthiazol-2-yl)-1,3-diphenylformazan (Formazan)

Fig. 1. The scheme of reducing the MTT reagent and obtaining formazan.

Table 1
The content of C, H, N, and Ni in **C1**, **C2**, **C3**, and **C4** complexes.

Complex	Nitrogen (%)		Carbon (%)		Hydrogen (%)		Nickel (%)	
	Exp.	Calc.	Exp.	Calc.	Exp.	Calc.	Exp.	Calc.
C1	14.82	15.01	36.13	36.05	4.58	4.75	12.87	12.58
C2	13.97	13.71	33.13	32.91	4.63	4.34	11.75	11.49
C3	17.51	17.69	35.89	35.40	4.12	4.24	12.07	12.36
C4	15.77	15.42	42.44	42.32	4.98	4.66	12.74	12.93

two water molecules (experimental loss, 8.12%; calculated loss, 7.72%). In the range of 180–280 °C, chlorine anion is lost as HCl (experimental loss, 7.67%; calculated loss, 7.82%). Ligand decomposition occurs in the third and fourth steps, with strong exothermic effects in the 280–450 °C range.

In case of complex **C2** up to approximately 200 °C, we have a mass loss of 7.50%, indicating the presence of two coordinating water molecules. In the range of 200–270 °C, bromine anion is lost as HBr (experimental loss, 16.25%; calculated loss, 15.85%). Above this temperature, the mass loss corresponds to the decomposition of the ligand being accompanied by exothermic effects.

Analyzing the TG and DSC curves of the **C3** complex, it is observed that in the first step (<180 °C) the crystallization water molecule is lost (experimental loss, 3.74%; calculated loss, 3.79%). Subsequently, the removal of nitrate ions as nitrogen oxides and oxidative degradation of the ligand takes place. Consequently, in the temperature range 400–500 °C, a strong exothermic effect can be observed.

The thermal analysis curves of the **C4** complex indicate that the acetate ion was eliminated as CO_2 and H_2O up to about 250 °C (experimental loss, 13.50%; calculated loss, 13.00%) and the ligand degradation takes place up to 500 °C.

For all four complexes analyzed, the residue obtained is NiO (greenish gray), from which the percentage of nickel was determined, namely, for **C1** (experimental, 12.73%; calculated, 12.58%), for **C2** (experimental, 11.28%; calculated 11.49%), for **C3** (experimental, 11.98%; calculated, 12.36%), and for **C4** (experimental, 13.42%; calculated, 13.00%). A good agreement was observed between the spectrophotometrically determined metal content and the corresponding value of the residue from thermal analysis.

3.3. Molar conductivity

All molar conductivities were determined at 25 °C using *N,N*-dimethylformamide as a solvent and concentrations of 10^{-3} M. The measured values for complexes are as follows: **C1**, 79.5; **C2**, 81.7; **C3**, 72.6; and **C4**, 77.2 S cm^2 mol^{-1}. These values indicate a 1:1 electrolyte type for all four complexes [22].

3.4. Magnetic susceptibility

Magnetic susceptibility determinations have led to the following magnetic moment values: 3.19 μB for **C1**, 3.27 μB for **C2**, and zero for both **C3** and **C4**. Consequently, the first two complexes are paramagnetic, whereas **C3** and **C4** complexes are diamagnetic.

3.5. Ultraviolet–visible–near-infrared spectra

The stereochemistry of synthesized coordination complexes has been assessed using ultraviolet, visible, and near-infrared (UV–vis–NIR) spectrometry by comparing their spectra to those of the ligands (α-ketoglutaric acid and 1-(*o*-tolyl)biguanide). The electron spectra of the solid state **C1**–**C4** complexes are shown in Fig. 3. The bands and the maxima assigned to the d–d transitions for the four synthesized complexes are shown in Table 2.

All complexes have absorption bands in the range of 230–345 nm that may me attributed to the π–π* and n–π* transitions of organic ligands H_2A and TB, slightly displaced by coordination of the ligand to metal ions.

The electronic spectra of the **C1** and **C2** complexes are very similar and correspond, by the position and intensity of the visible range bands, to a rhombic distorted octahedral symmetry [23].
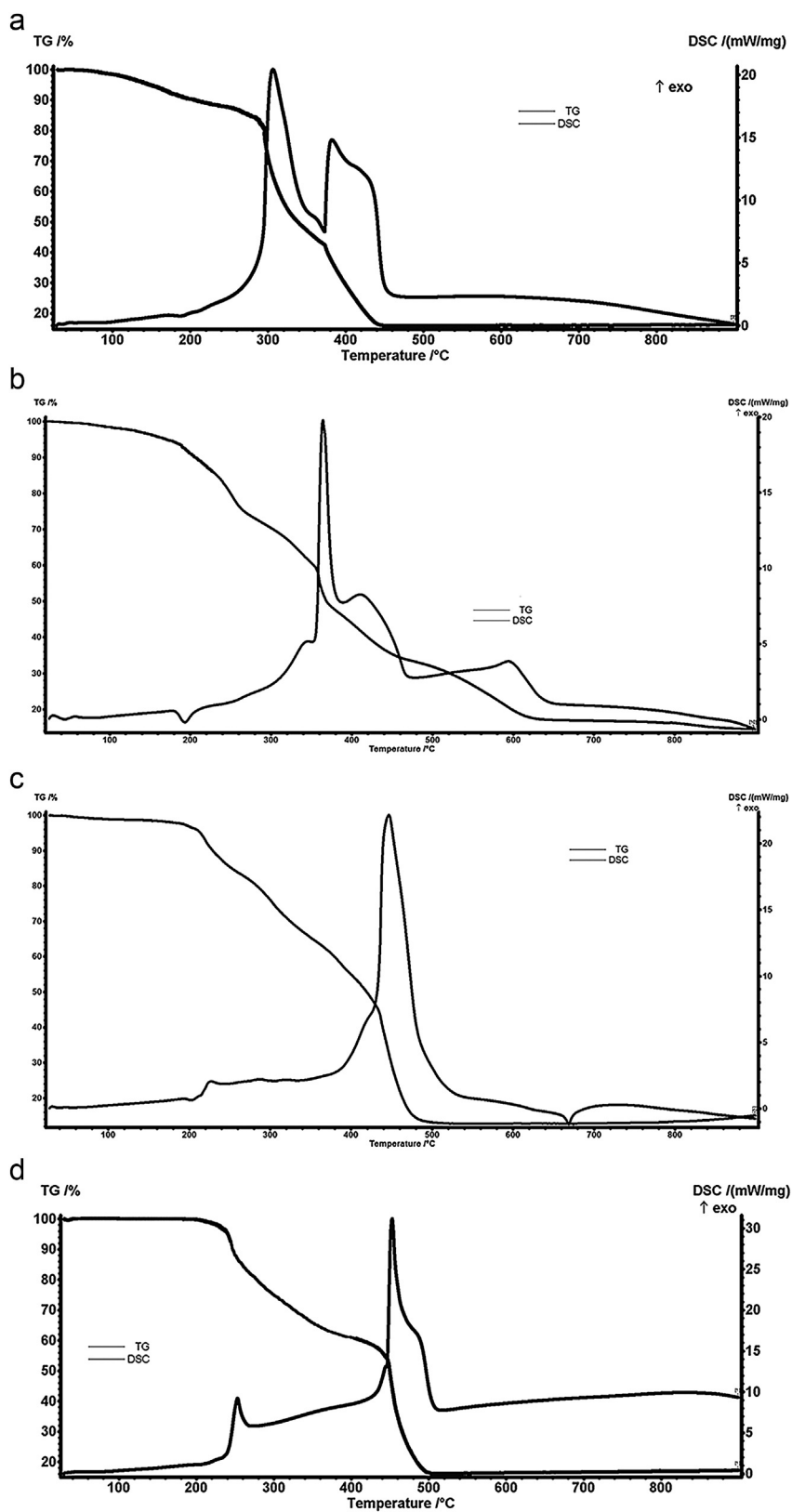
Fig. 2. TG and DSC curves of the complexes (a) [Ni(TB)(HA)(H$_2$O)$_2$]Cl, (b) [Ni(TB)(HA)(H$_2$O)$_2$]Br, (c) [Ni(TB)(HA)]NO$_3$·H$_2$O, and (d) [Ni(TB)(HA)]CH$_3$COO.
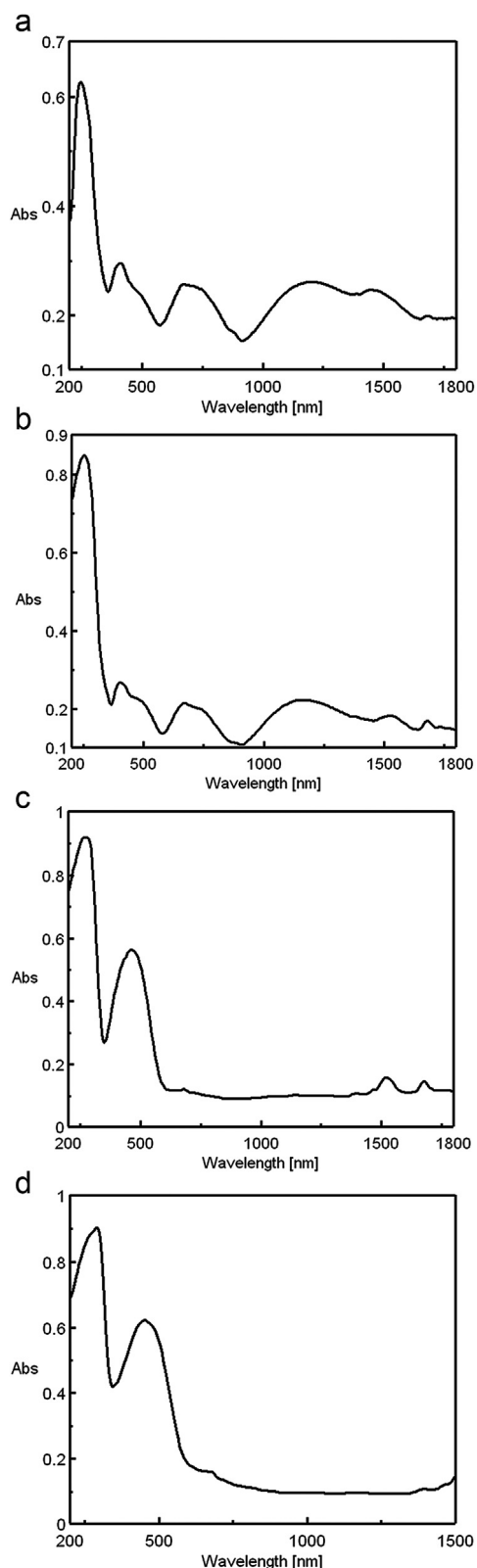
Fig. 3. The electronic spectra of the complexes (a) [Ni(TB)(HA)(H$_2$O)$_2$]Cl, (b) [Ni(TB)(HA)(H$_2$O)$_2$]Br, (c) [Ni(TB)(HA)]NO$_3$·H$_2$O, and (d) [Ni(TB)(HA)] CH$_3$COO.

Table 2
Maxima of d–d transition bands for **C1**–**C4** complexes.

Complex	Observed bands		Assignments	Symmetry
	λ_{max} (nm)	$\dot\nu$ (cm^{-1})		
C1	1200	8330	$^3B_1 \rightarrow {}^3A_1$	Rhombic
	750	13,330	$^3B_1 \rightarrow {}^3B_2$	distorted
	675	14,810	$^3B_1 \rightarrow {}^3B_2$ ($^3T_1$)	octahedral
	490	20,410	$^3B_1 \rightarrow {}^3A_2$ ($^3T_1$)	
	415	24,100	$^3B_1 \rightarrow A_2, {}^3B_1, {}^3B_2$ ($^3T_1/^3P$)	
C2	1155	8660	$^3B_1 \rightarrow {}^3A_1$	Rhombic
	745	13,420	$^3B_1 \rightarrow {}^3B_2$	distorted
	670	14,925	$^3B_1 \rightarrow {}^3B_2$ ($^3T_1$)	octahedral
	485	20,620	$^3B_1 \rightarrow {}^3A_2$ ($^3T_1$)	
	400	25,000	$^3B_1 \rightarrow A_2, {}^3B_1, {}^3B_2$ ($^3T_1/^3P$)	
C3	680	14,600	$^1A_{1g} \rightarrow {}^1A_{2g}$	Square-planar
	465	21,510	$^1A_{1g} \rightarrow {}^1B_{1g}$	
C4	680	14,710	$^1A_{1g} \rightarrow {}^1A_{2g}$	Square-planar
	450	22,220	$^1A_{1g} \rightarrow {}^1B_{1g}$	

The broad cleavage of the first and second octahedral bands cannot be explained on the basis of a tetragonal deformed octahedral symmetry. The existence of two different bidentate ligands in the plane and two water molecules in axial positions, that is, a chromophore NiO$_2$N$_2$O$_2$/2Ni–O (α-ketoglutaric acid), 2Ni–N (biguanide), and 2Ni–O(H$_2$O), leads to a rhombic deformation of the octahedron and a symmetry that corresponds, with good approximation, to C_{2v} [23]. Under these conditions, the bands of 8330/8660 and 13,330/13,420 cm^{-1} correspond to the transitions from the fundamental state $^3B_1$ to the terms $^3A_1$ and $^3B_2$ of the term $^3T_{2g}$ in the octahedral symmetry.

The other observed peaks that follow in the spectra correspond to the transitions to terms $^3B_2$ and $^3A_2$ from the $^3T_{1g}$(F) term of the octahedral symmetry. The cleavage of the third octahedral band that involves transitions to terms derived from the $^3T_{1g}$(P) level is not observed in any of the complexes. The position of all the observed bands is in agreement with the literature data regarding complexes having oxygen and nitrogen donor atoms and analogous symmetry [24–27].

C3 and **C4** complexes do not have bands below 10,000 cm^{-1} (which are characteristic of octahedral symmetry), their first bands being at 14,600 and 14,710 cm^{-1}, respectively.

The symmetry of these complexes is square-planar, in agreement with the observed diamagnetism and the fundamental term is $^1A_{1g}$. In agreement with the literature data, the observed peaks correspond to the first and second bands in D_{4h} symmetry (square-planar) [28–30].

The electronic spectra of the four complexes dissolved in DMSO were also recorded. It has been observed that the positions of the bands due to the metal ion do not change from those in the solid state, which means that the proposed symmetries are maintained. The electronic spectra of **C1**–**C4** complexes dissolved in DMSO are shown in Fig. 4.

3.6. FT-IR spectra

To determine the coordination mode of the ligands to the metal ion, the FT-IR spectra of the **C1**–**C4** complexes were compared with those of the H$_2$A and TB ligands [31].

The characteristic spectral bands and their assignments are shown in Table 3. To determine the coordination pattern of the H_2A ligand, the IR spectrum of sodium α-ketoglutarate was also analyzed, the difference between the wavelengths corresponding to the bands $\nu(COO^-)_{asym}$ and $\nu(COO^-)_{sym}$ being 181 cm^{-1}.

In the spectra of the four complex combinations, a band shift due to the valence vibration of the imine group, $\nu(C=N)$, from 1610 cm^{-1} to higher values is observed. This is in agreement with the coordination of the TB ligand to the metal ions through the lone pair of imine nitrogen. The displacement of this band to larger wavelengths is explained by the destruction of the π electron delocalization [32]. Coordination of 1-(o-tolyl)biguanide by iminic nitrogen atoms is also supported by the band displacement due to δ(NH) + ν(C−N) coupled vibration.

The displacement of the $\nu(C=O)$ band below 1720 cm^{-1} confirms that the keto group in the α position of the H_2A ligand is involved in the coordination for all the analyzed complexes.

From the difference between the corresponding wavenumbers of $\nu(COO^-)_{asym}$ and $\nu(COO^-)_{sym}$ bands (<181 cm^{-1}), it was established that the H_2A ligand coordinates with the metal ion in its deprotonated form HA^-, through α oxygen atom of the ketone group and the oxygen from the hydroxyl of the adjacent carboxyl group.

The presence of a single absorption band for the characteristic vibration modes $\nu_1-\nu_4$ in the **C3** complex spectrum indicates the presence of a nitrate anion in the ionization sphere.

In the **C4** complex, the intense bands at 1570 and 1410 cm^{-1} can be attributed to the out of the coordination sphere ionic acetate.

Bands between 260 and 270 cm^{-1} and 432 and 450 cm^{-1}, respectively, were assigned to the formation of Ni−O and Ni−N bonds.

The coordination water in the **C1** and **C2** complexes is confirmed by the presence of the three characteristic bands located at approximately 3400, 600, and 700 cm^{-1}. In the case of **C3** complex, the stretched band from 3370 cm^{-1} is attributed to the crystallization water.

3.7. Biological activity

Metabolism of HeLa cells varies depending on the type of the material used. Thus, ligands and **C1** and **C2** complexes show a very weak effect on HeLa tumor cells under the tested conditions, whereas complex **C3** and **C4** combinations have demonstrated a moderate cytotoxic effect on them. Fig. 5 shows the absorbance readings at 570 nm for the analyzed samples (at a concentration of 500 μg/mL for 24 h incubation at 37 °C) and untreated control sample indicating the metabolic activity of HeLa cell cultures by the MTT method.

Evaluation of the antimicrobial activity of the ligands and synthesized complexes was done on *S. aureus* and *P. aeruginosa* species. It has been observed that DMSO (the solvent used in dilutions) does not influence the antimicrobial activity of the tested compounds at the chosen working concentrations.

In the case of Gram-positive *S. aureus*, **C2** has shown identical activity to ligands, whereas **C1**, **C3**, and **C4**
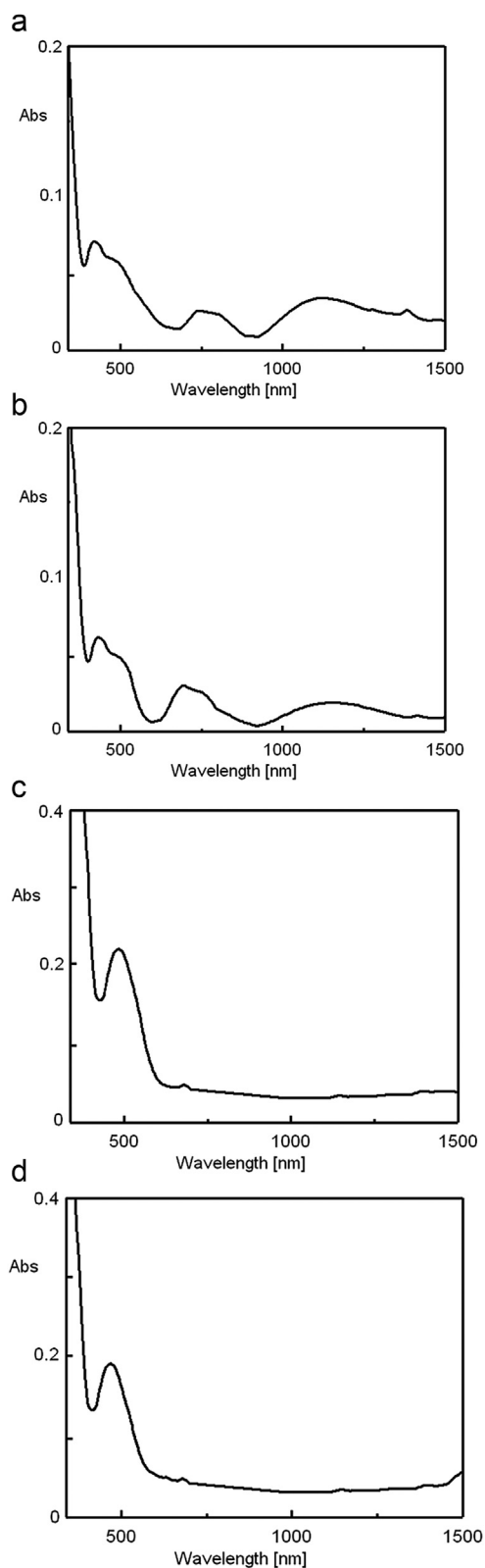

Fig. 4. The electronic spectra in DMSO of the complexes (a) [Ni(TB)(HA)(H$_2$O)$_2$]Cl, (b) [Ni(TB)(HA)(H$_2$O)$_2$]Br, (c)[Ni(TB)(HA)]NO$_3$·H$_2$O, and (d) [Ni(TB)(HA)]CH$_3$COO.

Table 3
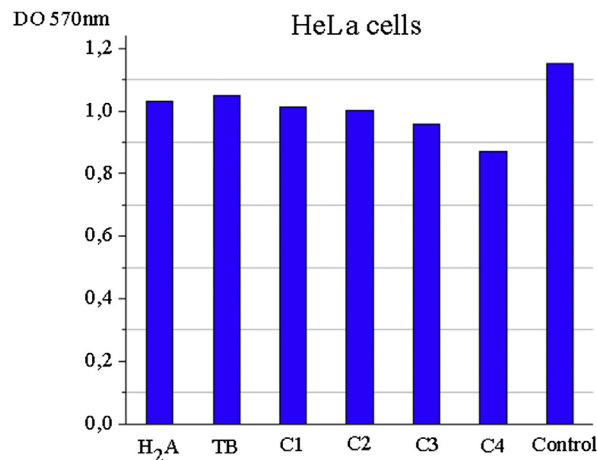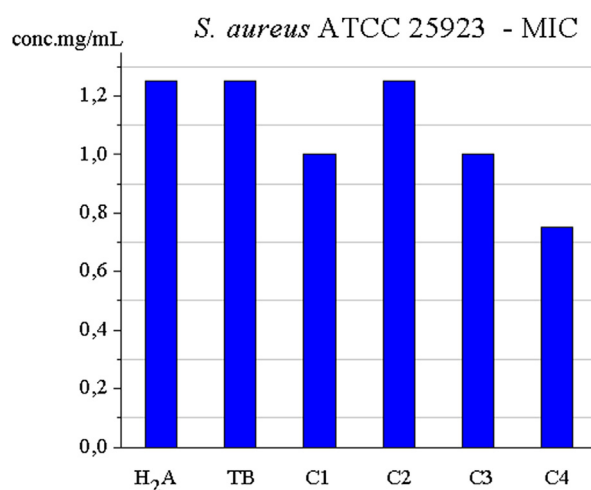IR bands and their assignments for the synthesized complexes and ligands.

Assignments	1-(o-Tolyl)biguanide	α-Ketoglutaric acid	C1	C2	C3	C4
$\nu(C=O)_{keto}$		1720vs	1690vs	1682vs	1695vs	1692vs
$\nu(C=N)$	1610vs		1635vs	1648vs	1660vs	1651vs
$\delta(NH) + \nu(C-N)$	1577m		1587m	1595m	1570m	1580m
	1270w		1252w	1257w	1255w	1244w
$\nu(COO^-)_{asym}$			1532vs	1544vs	1588vs	1595vs
$\nu(COO^-)_{sym}$			1387s	1392s	1445s	1432s
$\Delta = \nu_{(COO^-)asym} - \nu_{(COO^-)sym}$			145	152	143	163
$\nu_3(NO_3)$					1390vs	
$\nu_1(NO_3)$					1072m	
$\nu_2(NO_3)$					837m	
$\nu_4(NO_3)$					710s	
$\nu(C=O)_{acetate}$						1570s
$\nu(C-O)_{acetate}$						1410s
$\nu(Ni-N)$			450m	442m	432m	440m
$\nu(Ni-O)$			268m	270m	264m	260m
$\nu(OH)_{water}$			3390m	3410m	3370m	
$\rho_{r\ coord.\ water}$			780m	765m		
$\rho_{w\ coord.\ water}$			602s	617s		

s, strong, vs, very strong, m, medium, w, weak.

complexes show a better activity. Thus, **C4** has the best activity, whose MIC value is 0.75 mg/mL.

The activity of complexes synthesized (except **C2**) against Gram-negative bacteria *P. aeruginosa* is better for synthesized complexes than for H$_2$A ligand but similar to TB ligand. **C4** complex has the best activity among the tested substances against these bacteria (MIC is 1.00 mg/mL). MICs for the ligands and **C1**–**C4** complexes against the two bacterial strains are shown in Figs. 6 and 7.

Regarding the ability to inhibit the adhesion of the microbial biofilm to the inert substrate, in *S. aureus,* all the test compounds (ligands and complexes obtained) inhibit this process in a dose-dependent manner to a minimum biofilm eradication concentration of 0.04 mg/mL (**C3**, **C4**), 0.09 mg/mL (TB, H$_2$A, **C2**), and 0.18 mg/mL (**C1**). Against *P. aeruginosa*, all compounds have inhibitory capacity up to a minimum biofilm eradication concentration of 0.04 mg/mL (TB, **C1**–**C4**) and for H$_2$A of 0.09 mg/mL.

Fig. 6. MIC for **C1**–**C4** ligands against *S. aureus.*

Fig. 5. Absorbance values at 570 nm for ligands and complexes of HeLa cell cultures.
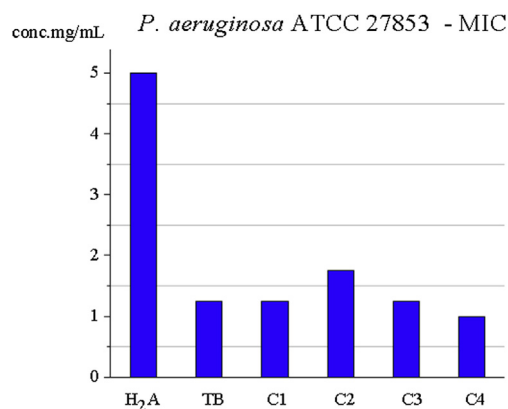
Fig. 7. MIC for **C1**–**C4** ligands against *P. aeruginosa.*
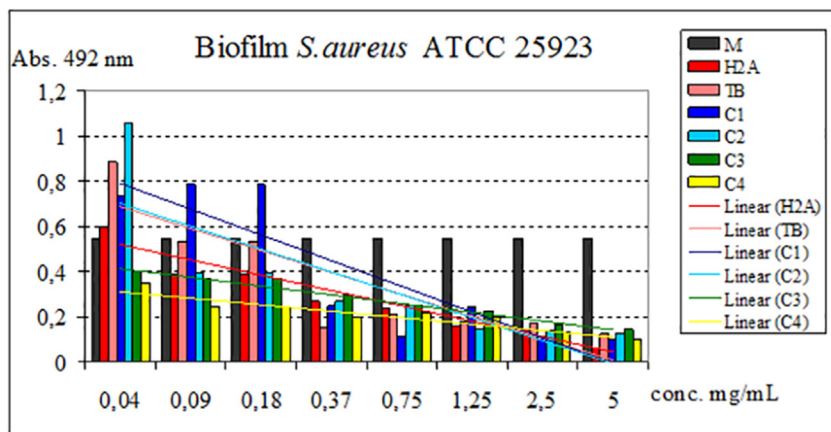
Fig. 8. Influence of H₂A, TB, and **C1**—**C4** on adhesion to the inert substrate of the strain *S. aureus*.

The influence of ligands and complexes on adhesion to inert substrate capacity is shown in Figs. 8 and 9.

4. Conclusions

Four nickel coordination complexes having α-ketoglutaric acid and 1-(*o*-tolyl)biguanide were synthesized and characterized.

On the basis of the analyses performed (elemental analysis, UV—vis—NIR spectra, IR, thermal analysis, molar electric conductance, and magnetic susceptibility), the formulas of **C1**—**C4** complexes were proposed.

Both α-ketoglutaric acid and 1-(*o*-tolyl)biguanide function as bidentate ligands in the four complexes (the structures of the two ligands) are shown in Fig. 10.

For the synthesized complexes, the following formulas for complex cations were proposed (Fig. 11a and b).

The antitumor activity in HeLa tumor cells of these complexes and the ligands used in the synthesis was tested. The best cytotoxic effect on this type of cell has the **C4**
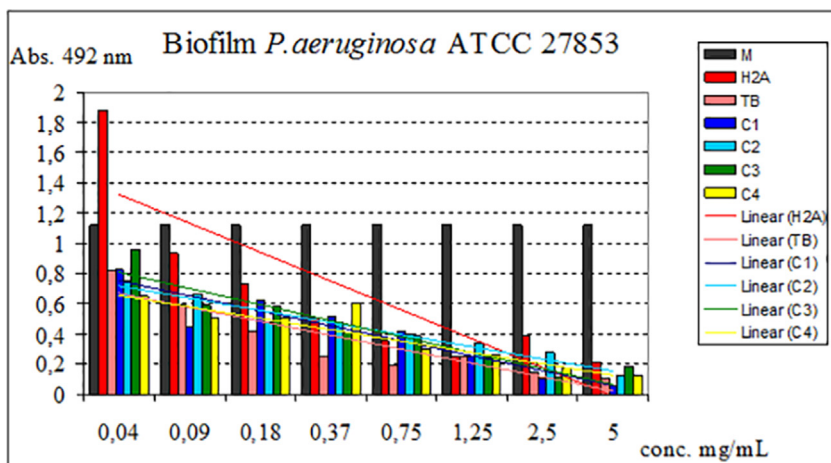

Fig. 9. Influence of H₂A, TB, and **C1**—**C4** on adhesion to the inert substrate of the strain *P. aeruginosa*.
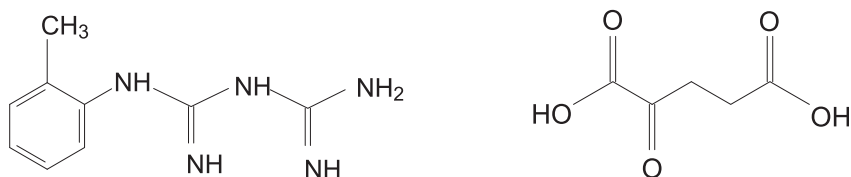

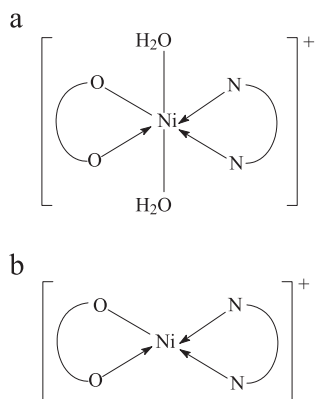**Fig. 10.** Structures of TB and H₂A ligands.

a

b

Fig. 11. Complex cation structure for (a) **C1** and **C2** and (b) **C3** and **C4**.

complex. Concerning the antibacterial activity of the synthesized complexes against *S. aureus* and *P. aeruginosa*, this is comparable or better than that of the ligands (**C3** and **C4** showing the best activity).

Because the **C1**−**C4** complexes are of the electrolyte type, their activity may result from the electrostatic interaction of the complex cation of these species with the negatively charged components of the cell membrane, consequently leading to their inactivation. On the other hand, antimicrobial activity may be associated with stereochemistry and the combined effect of the ligand and metal ion to inactivate a particular component involved in the pathogenesis of the microorganism.

The different activity of the **C1**−**C4** complexes can be attributed to their different stereochemistry. Better biological activity was observed for square-planar symmetry complexes (**C3** and **C4**) than octahedral (**C1** and **C2**).

Acknowledgment

References

[1] J.C.Z. Woo, V.G. Yuen, K.H. Thompson, J.H. McnNeill, C. Orvig, J. Inorg. Biochem. 76 (1999) 251−257.

[2] L. Patron, M. Giurginca, G.M. Patrînoiu, N. Iftimie, A. Meghea, Rev. Roum. Chim. 50 (6) (2005) 457−464.

[3] D. Sweeney, M.L. Raymer, T.D. Lockwood, Biochem. Pharmacol. 66 (2003) 663−667.

[4] C.J. Bailey, Diabetes Care 15 (6) (1992) 755−772.

[5] B. Viollet, B. Guigas, N. Sanz Garcia, J. Leclerc, M. Foretz, F. Andreelli, Clin. Sci. 122 (6) (2012) 253−270.

[6] M. Pollak, J. Clin. Invest. 123 (9) (2013) 3693−3700.

[7] A.M. Pelin, C.C. Gavat, G. Balan, C.V. Georgescu, Rev. Chim. (Bucharest) 64 (2) (2017) 378−379.

[8] M. Bogdan, I. Tica, D.N. Gheorghe, I. Silosi, S. Solomon, I. Martu, P. Surlin, I. Chiscop, C. Budacu, Rev. Chim. (Bucharest) 67 (12) (2016) 2651−2653.

[9] G. Patrînoiu, L. Patron, O. Carp, N. Stănică, J. Therm. Anal. 72 (2003) 489−495.

[10] M. Badea, A. Crasanda, M. Chifiriuc, L. Marutescu, V. Lazar, D. Marinescu, R. Olar, J. Therm. Anal. 111 (2013) 1743−1751.

[11] R. Olar, M. Badea, D. Marinescu, J. Therm. Anal. 99 (2010) 893−898.

[12] R. Olar, M. Badea, D. Marinescu, M. Iorgulescu, E. Frunza, V. Lazar, C. Chifiriuc, J. Therm. Anal. 99 (2010) 815−821.

[13] T. Joselin Beaula, P. Muthuraja, M. Sethuram, M. Dhandapani, V.K. Rastogi, V. Bena Jothy, J. Mol. Struct. 1128 (2017) 290−299.

[14] P. Grzesiak, M. Slupecko-Ziemilska, J. Wolinski, Dev. Period. Med. 20 (1) (2016) 61−67.

[15] D. Voet, J.G. Voet, Biochemistry, 4th ed., John Wiley & Sons, 2010, pp. 789−822.

[16] X. Yang, S. Bi, X. Wang, J. Liu, Z. Bai, Anal. Sci. 19 (2) (2003) 273−279.

[17] X.D. Yang, Z.P. Baii, S.P. Bi, B.Q. Li, Chin. J. Inorg. Chem. 18 (10) (2002) 981−986.

[18] M.D. Dulaney Jr., M. Brumley, J.T. Willis, A.S. Hume, Vet. Hum. Toxicol. 33 (6) (1991) 571−575.

[19] A.S. Hume, J.R. Mozingo, B. McIntyre, I.K. Ho, Clin. Toxicol. 33 (6) (1995) 721−724.

[20] V. Badea, T. Negreanu-Pîrjol, Arch. Balk. Med. Union 40 (3) (2005) 135−140. Celsius Publishing House.

[21] T. Negreanu-Pîrjol, A. Lepadatu, S. Jurja, R. Sirbu, R. Negreanu-Pîrjol, 15th International Multidisciplinary Scientific Geo-Conferences—SGEM, I, 2015, pp. 297−304.

[22] R.J. Angelici, Synthesis and Technique in Inorganic Chemistry, 3rd ed., Softbound, 1999, p. 254.

[23] A.B.P. Lever, Inorganic Electronic Spectroscopy, 2nd ed., Elsevier, 1984, pp. 517−519.

[24] A.B.P. Lever, I.M. Walker, P.J. McCarthy, Can. J. Chem. 69 (1982) 495.

[25] P.L. Meredith, R.A. Palmer, Inorg. Chem. 10 (1971) 1049.

[26] A.B.P. Lever, I.M. Walker, P.J. McCarthy, Inorg. Chim. Acta. 44 (1980) L143.

[27] M. Gerloch, I. Morgenstern-Badarau, J.-P. Audiere, Inorg. Chem. 18 (1979) 3220.

[28] A.B.P. Lever, J. Inorg. Nucl. Chem. 27 (1965) 149.

[29] C.K. Jorgensen, J. Inorg. Nucl. Chem. 24 (1962) 571.

[30] M.A. Hitchman, J.B. Bremner, Inorg. Chim. Acta 27 (1978) L61.

[31] K. Nakamoto, Infrared and Raman Spectra of Inorganic and Coordination Compounds, 3rd ed., John Wiley & Sons, 1978, pp. 230−232.

[32] S. Singh, R. Malhotra, K.S. Dhindsa, Proc. Natl. Acad. Sci. India 68A (1998) 217.